NASA Contractor Report 3574

Terminal Area Automatic Navigation, Guidance, and Control Research Using the Microwave Landing System (MLS)

Part 4 - Transition Path Reconstruction Along a Straight Line Path Containing A Glideslope Change Waypoint

Samuel Pines

CONTRACT NAS1-15116
JUNE 1982

NASA

NASA Contractor Report 3574

Terminal Area Automatic Navigation, Guidance, and Control Research Using the Microwave Landing System (MLS)

Part 4 - Transition Path Reconstruction Along a Straight Line Path Containing A Glideslope Change Waypoint

Samuel Pines
Analytical Mechanics Associates, Inc.
Hampton, Virginia

Prepared for
Langley Research Center
under Contract NAS1-15116

NASA
National Aeronautics
and Space Administration

Scientific and Technical Information Office

1982

TABLE OF CONTENTS

LIST OF FIGURES

LIST OF TABLES

SUMMARY

This report contains the algorithms necessary for constructing an aircraft flight path which contains a glideslope change at a waypoint which lies along a straight line. The report also contains the necessary algorithms to reconstruct the glideslope change waypoint along a straight line in the event the aircraft encounters a valid MLS update and transition in the terminal approach area.

Results of a simulation of the Langley B737 aircraft utilizing these algorithms are presented. The method is shown to reconstruct the necessary flight path during MLS transition resulting in zero cross track error, zero track angle error, and zero altitude error, thus requiring minimal aircraft response.

INTRODUCTION

Previous studies have shown the advantages of eliminating cross track, track angle and delta altitude errors through the method of a small path reconstruction at transition from TACAN to MLS navaids in the terminal area (Refs. 1, 2, and 3). These studies have been confined to a path which allowed vertical glideslope changes to occur only at the centers of turns. Since some terminal area flight paths require glideslope change to occur along a great circle (straight line) path, this study was undertaken to include glideslope change waypoints defined along straight line segments and to develop algorithms for updating these waypoints, at transition, in a manner consistent with the Continued Track Method outlined in Reference 3, in which the cross track error, the track angle error, and the vertical altitude error are all eliminated at the point of transition.

The algorithms are written in vector notation, consistent with the guidance and RNAV equation used in References 1, 2, and 3.

The report contains the derivation of the algorithms and the results of a computer study utilizing the equations for a variety of aircraft and runway landing conditions.

I. The Glideslope Change Waypoint Along a Straight Line

The input data required to define a great circle straight line on the Earth's surface consists of the latitude and longitude of two consecutive waypoints on that line. Thus, given λ_I, λ_{I+1}, δ_I and δ_{I+1}, we have

$$\hat{WR}(1) = \begin{Bmatrix} \sin(\delta_I) \\ -\cos(\delta_I)\sin(\lambda_I) \\ \cos(\delta_I)\cos(\lambda_I) \end{Bmatrix} \tag{1}$$

and

$$\hat{WR}(2) \quad \begin{Bmatrix} \sin(\delta_{I+1}) \\ -\cos(\delta_{I+1})\sin(\lambda_{I+1}) \\ \cos(\delta_{I+1})\cos(\lambda_{I+1}) \end{Bmatrix} \tag{2}$$

The unit normal, $\hat{WN}(I)$, perpendicular to the plane of the great circle which contains $\hat{WR}(I)$ and $\hat{WR}(I+1)$ is given by

$$\hat{WN}(I) = \frac{\hat{WR}(I) \times \hat{WR}(I+1)}{\left|\hat{WR}(I) \times \hat{WR}(I+1)\right|} \tag{3}$$

The difficulty in defining the input data for three consecutive waypoints, each of which is to be required to lie in the same great circle plane, is that one has to solve a nonlinear equation for the intermediate latitude and longitude of the middle waypoint. In order to simplify the input data requirements, it is sufficient to input an approximate latitude and an approximate longitude for the interior point not necessarily on the line, plus a numerical index identifying a glideslope change waypoint. The path generation algorithm, stored in the computer memory, will automatically relocate the approximate waypoint, $\hat{WR}(I+1)$, associated with proper index, on to the great circle, utilizing the cross track error algorithm for finding the desired unit vector, $\hat{WD}$, on a

great circle path, given the unit waypoint, $\hat{WR}(I+1)$, and the unit normal, $\hat{WN}(I)$, defined by the vector cross product of $\hat{WR}(I)$ and $\hat{WR}(I+2)$.

The index recommended for use in this report is to define the radius of desired circle, $R_T(I)$, associated with glideslope change waypoint, $\hat{WR}(I+1)$, to be zero.

Thus, in computing the unit normal, Equation (3), between two successive waypoints, if the radius of the turn circle, $R_T(I)$, associated with the waypoint $\hat{WR}(I+1)$ is equal to zero (0.), the algorithm for determining the unit normal is given by,

$$\text{If, } R_T(I) = 0. \tag{4a}$$

then

$$\hat{WN}(I) = \frac{\hat{WR}(I) \times \hat{WR}(I+2)}{\left|\hat{WR}(I) \times \hat{WR}(I+2)\right|} \tag{4b}$$

and the relocated glideslope change waypoint, $\hat{WR}(I+1)$ becomes

$$\hat{WD} = \frac{1}{\cos b}\left\{\hat{WR}(I+1) - \sin b\ \hat{WN}(I)\right\} \tag{5a}$$

where

$$\cos b = \hat{WR}(I+1) \cdot \hat{WN}(I)$$

and

$$\sin b = \sqrt{1 - \cos^2 b} \tag{5b}$$

Finally, if the radius of the turn, $R_T(I)$, associated with the glideslope change waypoint, $\hat{WR}(I+1)$, is zero, we determine the unit normal, $\hat{WN}(I+1)$, to be equal to the previous unit normal, $\hat{WN}(I)$. Thus,

$$\text{if, } R_T(I) = 0. \tag{6a}$$

Then

$$\hat{WN}(I+1) = \hat{WN}(I) \tag{6b}$$

The only additional change that is required in the algorithm for path construction is to set the required turn angle, ψ (I) , associated with the glideslope change waypoint, $\hat{WR}(I)$, whose radius, $R_T(I)$, is equal to zero. Thus,

If, $$R_T(I) = 0. \tag{7a}$$

Then, $$\psi(I) = 0. \tag{7b}$$

This is required because the computation for the turn angle, ψ (I), is obtained by means of an arc tangent routine, and some round off inaccuracies could result in a setting $\psi(I)$ equal to some small angle, thus producing an error in the distance to go logic.

The geometric equivalent of Equations (4b), (5a), and (6b) are shown in Figure 1.

For a normal first interior waypoint, containing a finite non-zero turn radius, $R_T(1)$, the path generation algorithms will produce two contiguous segments. The first segment is a great circle (straight line) beginning at the initial unit waypoint, $\hat{WR}(1)$, and terminating at the first incoming unit tangent vector, $\hat{PI}(1)$, which marks the start of the turn. The second segment is the first half of the turn about the first unit center turn vector, $\hat{CR}(1)$. This segment starts at $\hat{PI}(1)$ and terminates at the middle of the turn, marked by the unit vector , $\hat{WC}(1)$. The logic for changing glideslope is restricted to discontinuities at these unit middle of the turn vectors, $\hat{WC}(I)$.

For a normal path generation sequence, arising from the first turn to the second turn, the existing algorithms will create three segments. The first segment is the second half of the first turn, starting at $\hat{WC}(1)$ and terminating at the outgoing unit tangent vector, $\hat{PI}(2)$. The second segment is a great circle beginning with $\hat{PI}(2)$ and terminating at the start of the second turn, the unit incoming tangent vector $\hat{PI}(3)$. The final, third segment is the

first half of the second turn about the second unit center of turn vector, $\hat{CR}(2)$ associated with the turn radius, $R_T(2)$.

By using the zero magnitude of the turn radius, associated with the glideslope change waypoint, as the index, we are able to retain all the above logic without change. Thus,

If, $R_T(I) = 0.$ (8a)

The existing algorithms will automatically set the required unit vectors equal to one another.

$$\hat{PI}(2I-1) = \hat{WC}(I) = \hat{PI}(2I) = \hat{CR}(I) = \hat{WR}(I) \quad (8b)$$

In this manner, the existing logic for providing for glideslope discontinuities at the middle of each turn, the glideslope change waypoint, $\hat{WR}(I)$, will automatically be provided for. See Figure 2.

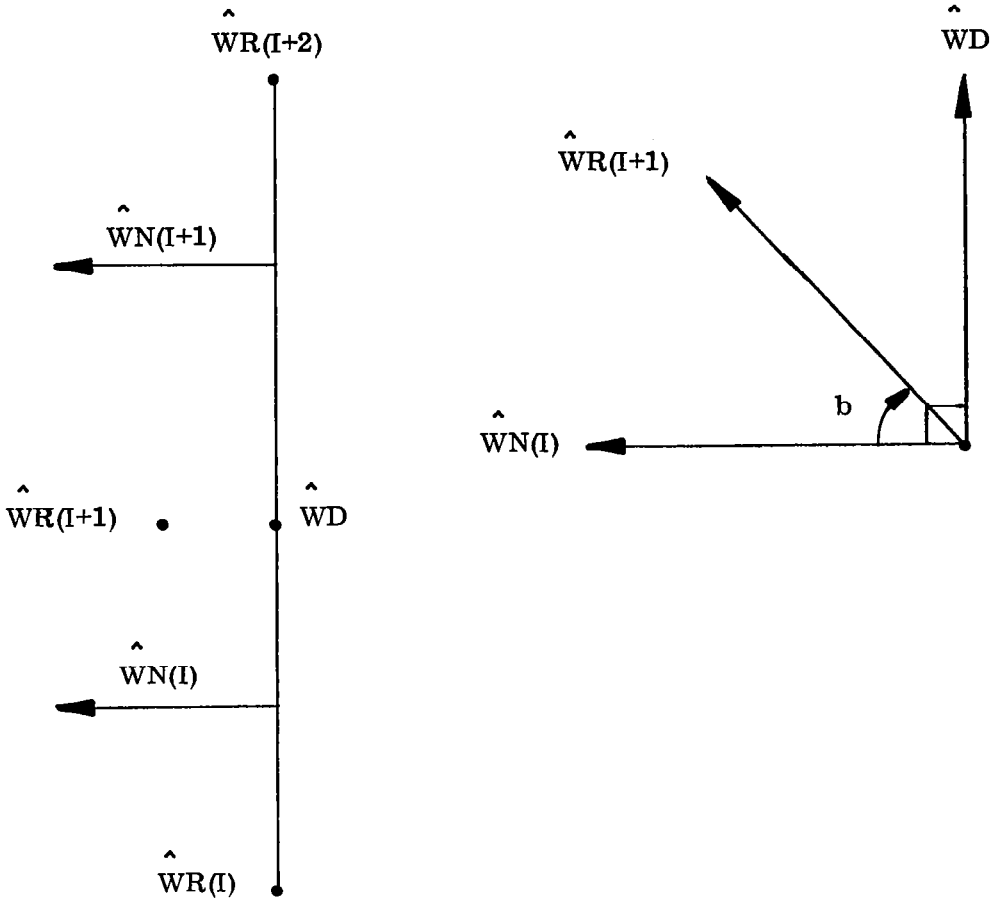

Figure 1.—Path construction for a glideslope waypoint on a great circle.

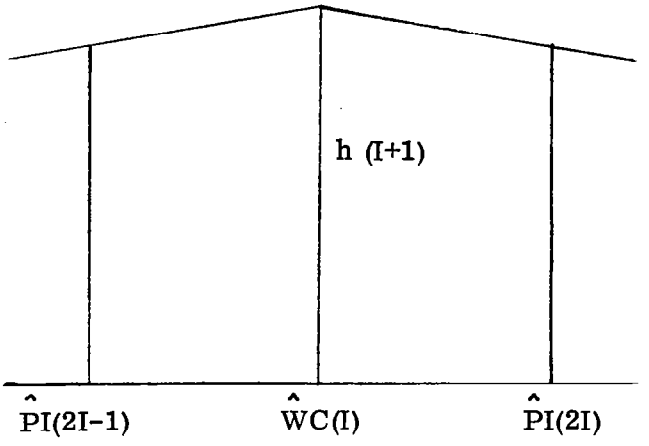

Figure 2(a).—Glideslope change for RT(I) > 0.

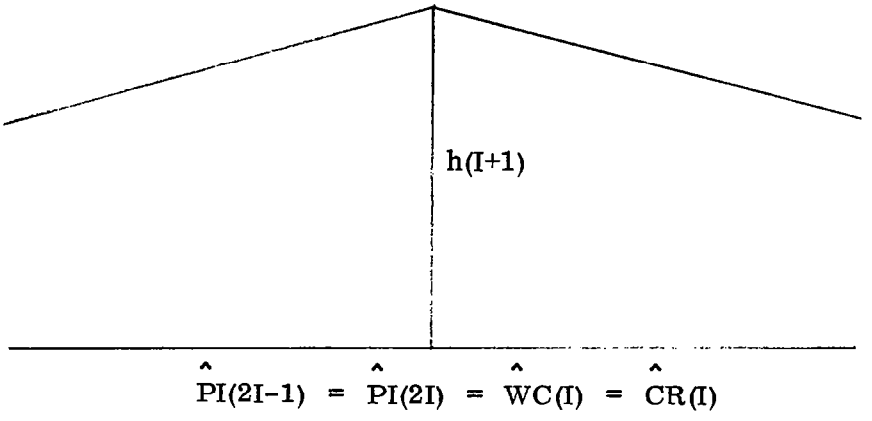

Figure 2(b).—Glideslope change for RT(I) = 0.

II. Glideslope Change Waypoint Reconstruction Following Valid MLS Transition

We assume that at the onset of a valid MLS, we are traversing a great circle path (straight line) containing an oncoming glideslope change waypoint. Utilizing the transition logic for the Continued Track, (Ref. 3), we set

Utilizing existing RNAV equations, based on the MLS update, we may obtain the aircraft latitude, δ (MLS), longitude, λ (MLS), and altitude, h (MLS). We now set our first bulk storage waypoint data to be

$$\begin{aligned} \lambda\,(1) &= \lambda(\mathrm{MLS}) \\ \delta\,(1) &= \delta(\mathrm{MLS}) \\ h\,(1) &= h(\mathrm{MLS}) \\ \mathrm{IC}\,(1) &= 0 \\ \mathrm{VG}\,(1) &= \mathrm{VG(RNAV)} \end{aligned} \tag{9a}$$

This defines the first waypoint to be

$$\hat{W}R(1) = \begin{Bmatrix} \sin(\delta_{MLS}) \\ -\cos(\delta_{MLS})\sin(\lambda_{MLS}) \\ \cos(\delta_{MLS})\cos(\lambda_{MLS}) \end{Bmatrix} \tag{9b}$$

This provides zero cross track error. The RNAV equations yield the velocity of the aircraft relative to the rotating Earth, in inertial coordinates, $\dot{R}_E(t)$. The unit normal, $\hat{W}N(1)$, is computed in the same fashion as in Reference 3 for the Continued Track

$$\hat{W}N(1) = \frac{\hat{W}R(1) \times \dot{R}_E(t)}{\left|\hat{W}R(1) \times \dot{R}_E(t)\right|} \tag{9c}$$

This guarantees zero track angle error.

Since we have assumed that we are on a great circle and that the next waypoint is a glideslope change waypoint, the radius of next waypoint will be zero.

If

$$R_T(I) = 0. \tag{9d}$$

then we set into bulk data

$$R_T(1) = R_T(I) \tag{9e}$$

and

$$\begin{aligned} \lambda(2) &= \lambda(I+1) \\ \delta(2) &= \lambda(I+1) \\ IC(2) &= 0 \\ VG(2) &= VG(I+1) \end{aligned} \tag{9f}$$

Before accepting the altitude of glideslope change waypoint, h(I+1), we must first test to see if we are too close to the oncoming waypoint. This is necessary since we wish to avoid a double change in glideslope over a short time interval.

Given the existing normal, $\hat{WN}(1)$ and the latitude and longitude of the next waypoint, we have

$$\hat{WR}(2) = \begin{Bmatrix} \sin\left(\delta(2)\right) \\ -\cos\left(\delta(2)\right)\sin\left(\lambda(2)\right) \\ \cos\left(\delta(2)\right)\cos\left(\lambda(2)\right) \end{Bmatrix} \tag{10}$$

The desired location of $\hat{WR}(2)$ on the Continued Track great circle is given by Equations 5(a) and 5(b).

$$\hat{WD} = \frac{1}{\cos b}\left\{\hat{WR}(2) - \sin b\ \hat{WN}(1)\right\} \tag{11a}$$

where

$$\begin{aligned} \cos b &= \hat{WR}(2) \cdot \hat{WN}(1) \\ \sin b &= \sqrt{1 - \cos^2 b} \end{aligned} \tag{11b}$$

To obtain the distance to go from $\hat{WR}(1)$ to $\hat{WD}$, we have

$$DIST = R_E * \left(\sin^{-1} \left(\left| \hat{WR}(1) \times \hat{WD}(1) \right| \right)\right) \tag{12}$$

If

$$DIST \geq VERLIM$$

$$h(2) = h(I+1) \tag{13a}$$

If

$$DIST < VERLIM$$

$$h(2) = h(1) + GRAD(I) * DIST \tag{13b}$$

A typical value for VERLIM is 1 kilometer, which is preset in data bulk storage. See Figure 3.

The remainder of the bulk storage required for path reconstruction is identical to that given in Reference 3 for the Continued Path Construction.

Finally, a change in the logic for calling in the next segment is required if we have come to the end of the great circle segment and the next waypoint is a glideslope change waypoint or a great circle.

If the time to go, TOGO, is triggered and $R_T(I) = 0.$, then we update the segment counter by three, in order to skip over the three interior segments associated with the zero turn angle.

III. Simulation Study of the Glideslope Change Waypoint Reconstruction

A. Description of the Simulation Test Data

This section contains computer generated plots of computer runs carried out using the FILCOMP program. The FILCOMP program was augmented to provide the algorithms described in Section I and II of this report to permit for the inclusion of interior waypoints at which glideslope changes occur along a straight line segment. Each run consists of three sets of plots.

The first half-page in each series contains a plot of the aircraft ground track illustrating the original and reconstructed paths. The original waypoint data point is indicated by a point enclosed by a diamond. The reconstructed waypoint is marked by a point contained in a circle. The glideslope change waypoint is indicated by a point enclosed in a diamond (or a circle) and may be recognized by the fact that it occurs along a straight line segment of the ground track. The boundary limit of the MLS azimuth antenna are marked by a dashed line emanating from the azimuth antenna. The boundary limit of the elevation antenna is illustrated by a dashed line emanating from the antenna site to the right of the beginning of the runway. The initial point at the start of each trajectory is indicated by a point enclosed in a diamond. In some instances this may occur too far away to be contained on the plot.

Transition occurs immediately after all three MLS signals are received valid. The last to come in is usually the elevation signal and transition occurs when the ground track and the elevation boundary intersect. Since this series of simulation runs is designed to illustrate the path reconstruction for glideslope change waypoints occurring on a straight line segment, the reconstructed glideslope change waypoint will be found adjacent to the original waypoint along the straight line segment when the vertical path slope discontinuity occurs.

The cases investigated in this series include:

(1) Glideslope change waypoint reconstruction on the first leg with a short distance to go.

(2) Glideslope change waypoint reconstruction on the first leg with a distance to go greater than VERLIM.

(3) Glideslope change waypoint reconstruction between two turns.

(4) Glideslope change waypoint reconstruction on the last straight line segment leading to the touchdown.

The second half of the first page in each series contains a plot of the altitude (meters) time history from the initial time to touchdown.

The second page of each case consists of seven plots of pertinent data as a function of time. These consist of the following:

(1) Glide path deviation in meters for both the true deviation and the estimated deviation for the particular navigation filter in use in the guidance loop for aircraft control.

(2) Aircraft pitch angle in degrees for the true pitch, the measured pitch output of the IMU (used in the complementary filter) and the estimated pitch corrected for the estimated gyro drift bias (used in the Kalman filter output).

(3) Aircraft altitude rate, measured in meters per second, for both the true rate of climb and the estimated rate obtained by the particular filter supplying the control system equations.

(4), (5), (6) Errors in the estimate of the forward, lateral, and vertical coordinates of the aircraft measured in the flat Earth runway coordinate system for both the Kalman and the complementary filters, measured in meters.

(7) Error in the estimate of the forward velocity component, $\hat{\dot{x}}_{1R}$, in the runway coordinate system, measured in meters per second for both the complementary and the Kalman filters.

The third and last page of each series contains eight plots of data as a function of time. These consist of the following:

(1) Cross track error, measured in meters, for both the true CRTE and the estimated CRTE obtained by the navigation filter used to supply the guidance equations.

(2) Track angle error, converted from degrees to the time rate of change of cross track error by multiplying by the ground speed. Both the true track angle error and the estimated track angle error supplying the guidance equations are shown, measured in meters per second.

(3) Aircraft roll angle, measured in degrees, for the true roll angle, the measured roll angle supplying the complementary filter, and the measured roll angle corrected for the gyro drift bias (used in the Kalman filter estimate of the aircraft roll angle).

(4) Error in the north complement of the wind, in meters per second, for both the Kalman and the complementary filters.

(5) Error in the estimate of the west component of the wind, in meters per second, for both the Kalman and the complementary filters.

(6) Difference between the true desired airspeed and the true airspeed. A second plot also shows the difference between the true ground speed and the true airspeed. The curves are mirror images of one another in the event the winds are zero, and differ in the presence of finite winds.

(7) Error in the estimate of the lateral velocity component, $\hat{\dot{x}}_{2R}$, in the runway coordinate system, measured in meters per second for both the Kalman and the complementary filters.

(8) Error in the estimate of the vertical velocity component, $\hat{\dot{x}}_{3R}$, in the runway coordinate system, measured in meters per second, for both the Kalman and the complementary filters.

B. Discussion of the Results

Five cases are studied in this report. The first two illustrate the ability of the method to construct and to reconstruct a glideslope change on the initial straight line segment on the approach to the terminal area. The first case, Figures 3(a), 3(b), and 3(c) illustrates the behavior of the aircraft in going from level flight to a 3^{o} glideslope descent under the condition that

the VERLIM distance is only 60.96 meters, (200 ft). With this small tolerance the original altitude is left unchanged, and the aircraft attempts to execute two changes in glideslope in a very short period of time, (1^{o} sec). The effect is indicated in Plot 1, the glideslope deviation, in Figure 3(b). The same extreme behavior is indicated in Plot 3, of Figure 3(b), the time rate of change of altitude reaches a peak value of -10 m/sec (32.81 ft/sec).

Case 2 illustrates the same approach conditions with a VERLIM of 914.4 meters (3000 ft). Here, the distance to the approaching glideslope change waypoint is less than the VERLIM setting, and the altitude for the oncoming waypoint, at transition, is reset to maintain the initial zero glideslope, so that only one change in glide occurs. Plot 1 (Fig. 4(b)) shows a large reduction in glideslope deviation, and Plot 3 (Fig. 4(b)) shows a maximum altitude rate of 7 m/sec (21.4 ft/sec). Comparison of Case 1 and 2 illustrates that a VERLIM of approximately 1000 meters (3280.8 ft) provides a comfortable transition and glideslope reconstruction along a straight line segment.

Case 3, Figures 5(a), 5(b),and 5(c) illustrate the ability to construct, and to reconstruct, a glideslope change waypoint along an intermediate straight line segment lying between two turns in the terminal area. Here, again, a VERLIM of 814.4 meters (2482.2 ft) is sufficient to provide a comfortable transition following the first valid MLS update along the intermediate straight line segment. Plot 3 of Figure 5(b) shows a maximum of 6 m/sec (18.3 ft/sec) vertical velocity required to achieve the change from zero glideslope to the 3^{o} glideslope descent.

Case 4, Figures 6(a), 6(b), and 6(c) illustrate that going to a larger value of VERLIM, 1524 meters (5000 ft) produces very little additional improvement in the response of the aircraft at transition to the required change in glideslope for landing.

Case 5, Figures 7(a), 7(b), and 7(c) illustrate the capability of the method to design a more complicated landing approach pattern in which a change from 3^{o} descent to a zero ($0.^{o}$) glideslope is required just prior to landing in order to avoid some obstacle. Here, the straight line segment along which the glideslope change occurs is the final leg immediately prior to touchdown. The method is seen to produce the required vertical path (Fig. 7(a)).

References

1. Pines, S.; Schmidt, S. F.; and Mann, F.: Automated Landing, Rollout, and Turnoff Using MLS and Magnetic Cable Sensors. NASA CR-2907, 1977.

2. Pines, S.: Terminal Area Automatic Navigation, Guidance, and Control Research Using the Microwave Landing System (MLS). Part 2 - RNAV/MLS Transition Problems for Aircraft. NASA CR-3511, Jan. 1982.

3. Pines, S.: Terminal Area Automatic Navigation, Guidance, and Control Research Using the Microwave Landing System (MLS). Part 3 - A Comparison of Waypoint Guidance Algorithms for RNAV/MLS Transition. NASA CR-3512, Jan. 1982.

TABLE I

VORTAC AND MLS STATION COORDINATES

VORTAC STATION COORDINATES

STATION LONGITUDE	40.40316
STATION LATITUDE	-27.164894
STATION ALTITUDE	45.72 m

MLS STATION COORDINATES

AZIMUTH & DME LONGITUDE	40.25
AZIMUTH & DME LATITUDE	-77.025
AZIMUTH & DME ALTITUDE	0.

ELEVATION DISTANCE FROM RUNWAY COORDINATE FRAME ORIGIN

XEL(1) = 1000., XEL(2) = 254.78, XEL(3) = .47

RUNWAY HEADING = 30 ^{o}

TABLE II

INPUT DATA FOR WAYPOINT CONSTRUCTION

CASES 1 and 2

N = 5

I	λ (I) Deg	δ (I) Deg	h (I) m	V_D(I) m/sec	IC	R_T(I) m
1	-77.1453838	40.29759451	840.03	74.594	0	0.
2	-77.1394011	40.27189941	840.03	74.594	0	2286.
3	-77.13148869	40.23788553	640.811	69.449	0	1524.
4	-77.0584522	40.20574384	290.748	64.305	0	—
5	-77.02320521	40.25237254	0.	64.305	0	—

TABLE III

INPUT DATA FOR WAYPOINT CONSTRUCTION

CASES 3 and 4

N = 5

I	λ (I) Deg	δ (I) Deg	h (I) m	V_D(I) m/sec	IC	R_T(I)
1	-77.14538380	40.29759451	490.118	74.594	0	2286.
2	-77.13148869	40.23798553	490.118	74.594	0	0
3	-77.10196103	40.2249002	490.118	69.449	0	1524.
4	-77.05845224	40.20574384	290.748	64.305	0	—
5	-77.02320521	40.25237254	0.	64.305	0	—

TABLE IV

INPUT DATA FOR WAYPOINT CONSTRUCTION

CASE 5

N = 5

I	λ (I) Deg	δ (I) Deg	h (I) m	V_D(I) m/sec	IC	R_T(I)
1	-77.1453830	40.29759451	762.00	74.594	0	2286.
2	-77.13148869	40.23788553	548.64	74.594	0	1524.
3	-77.05845224	40.20574384	195.07	64.305	0	0.
4	-77.04500673	40.22353989	195.07	64.305	0	—
5	-77.02320521	40.25237254	0.	64.305	0	—

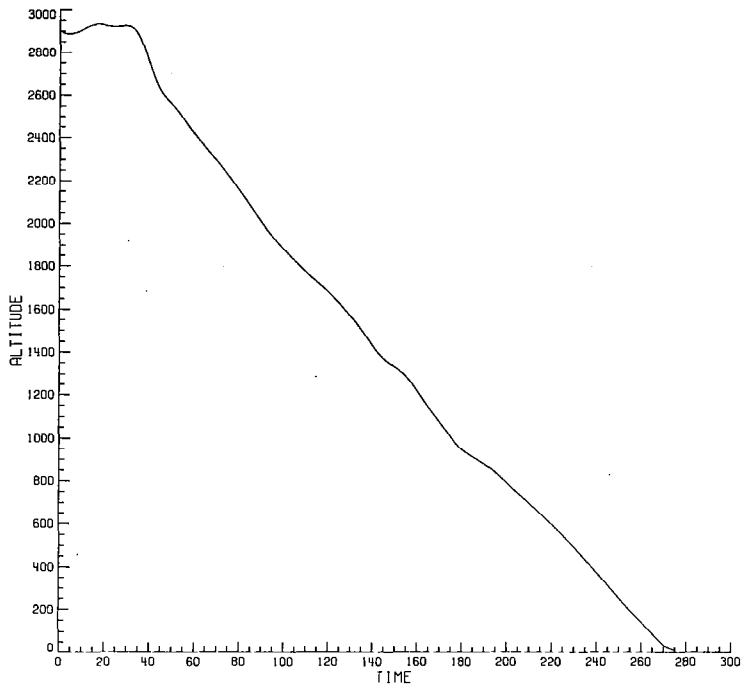

VERLIM = 60.96 m

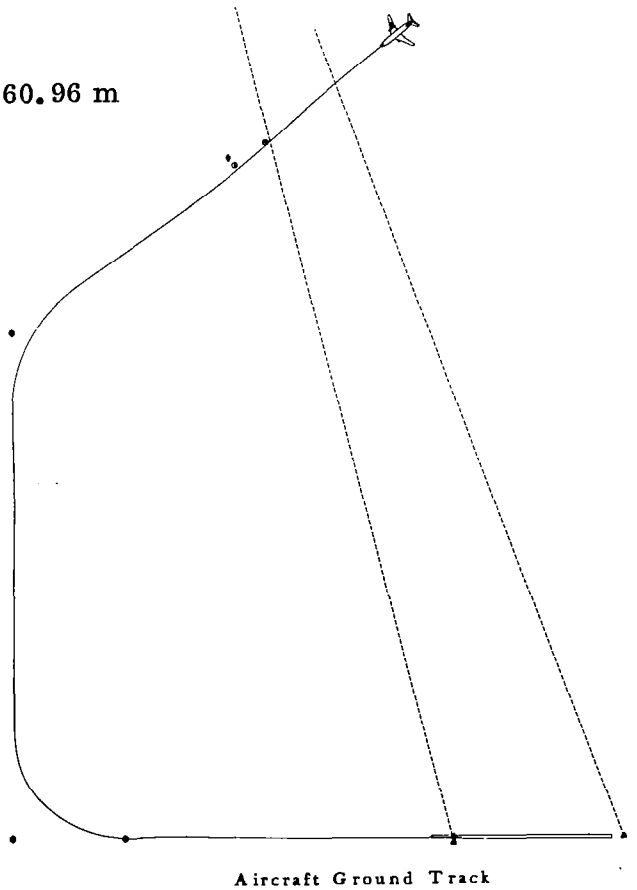

Final Distance = 2.41 Nautical Miles

Figure 3(a). - Case 1.

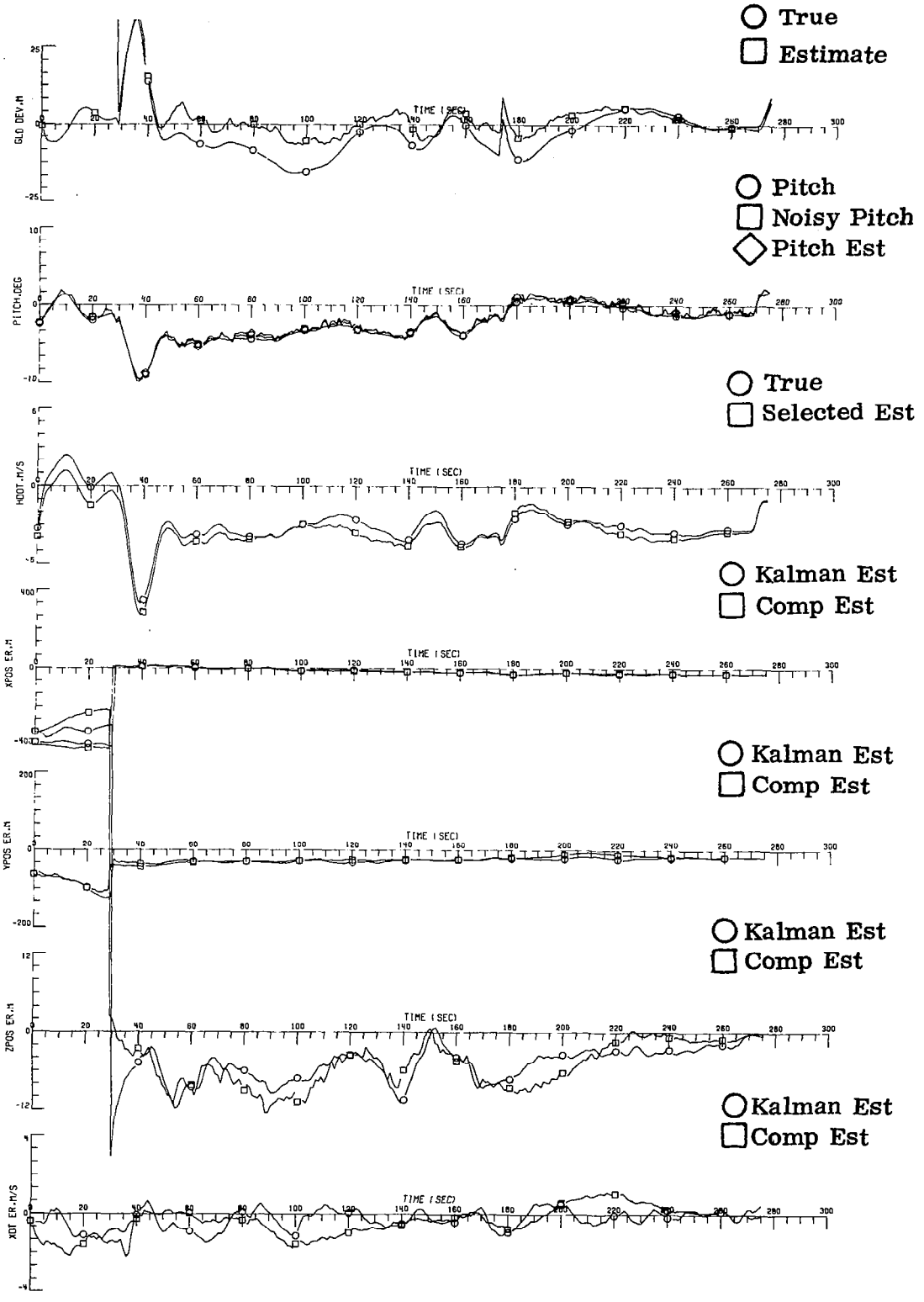

Figure 3(b). - Case 1.

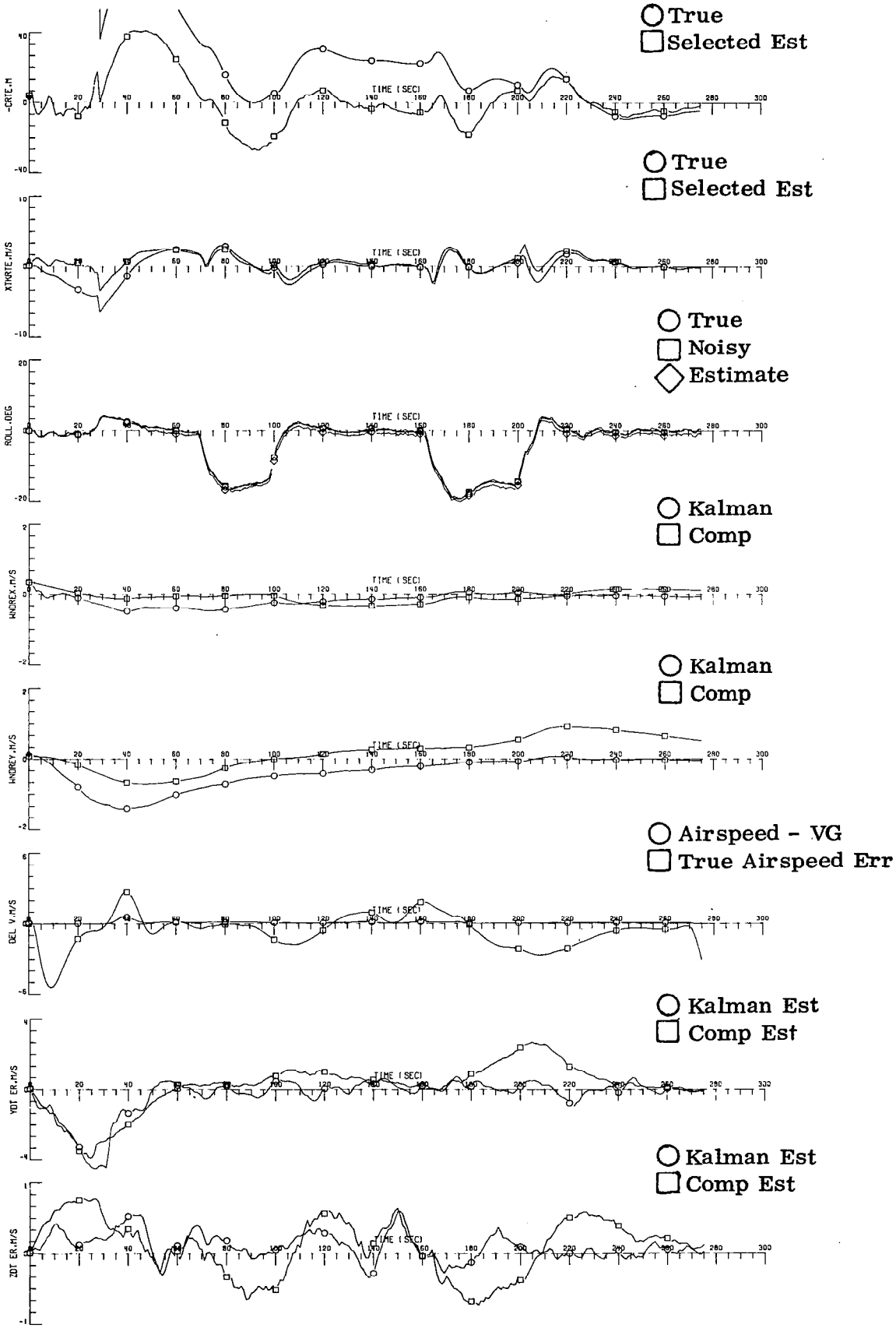

Figure 3(c). - Case 1.

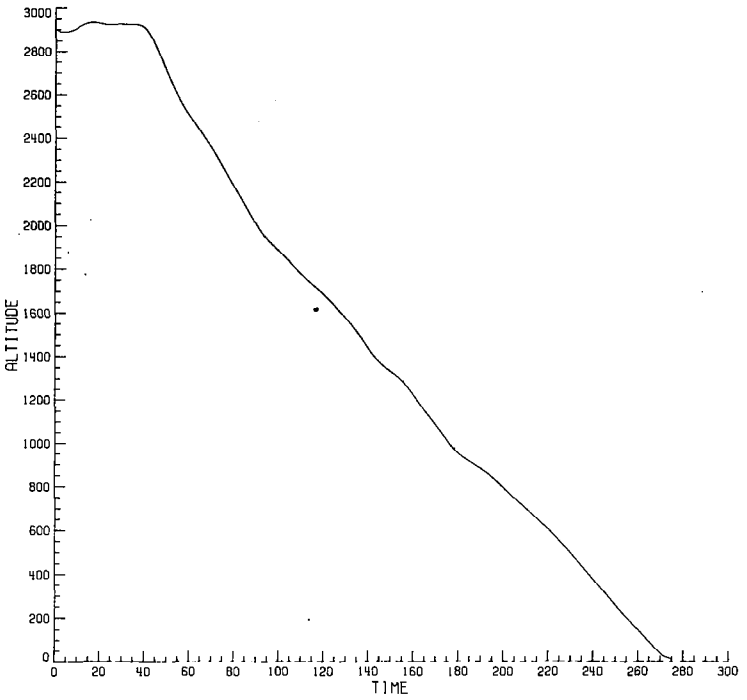

VERLIM = 914.4 m

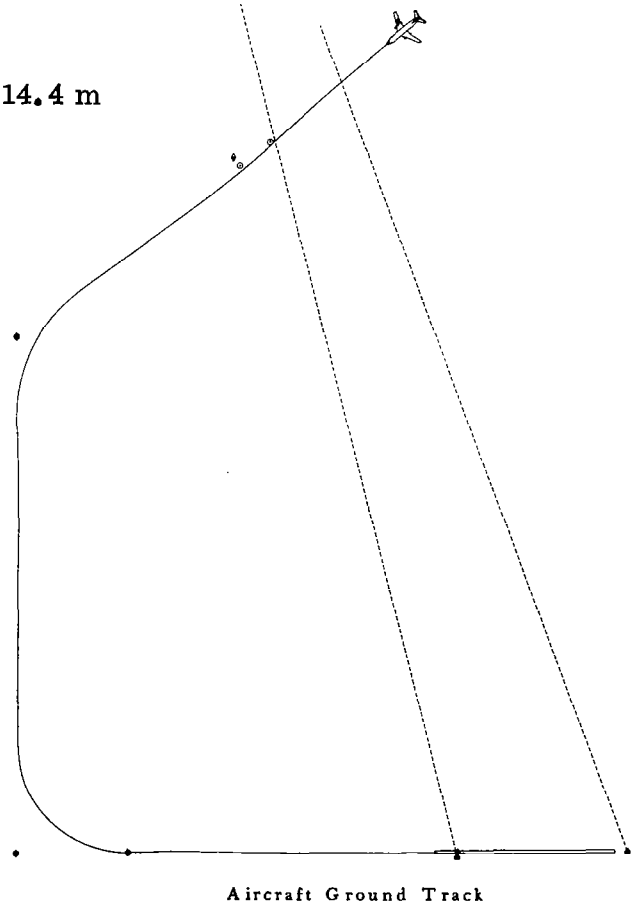

Aircraft Ground Track

Final Distance = 2.41 Nautical Miles

Figure 4(a). - Case 2.

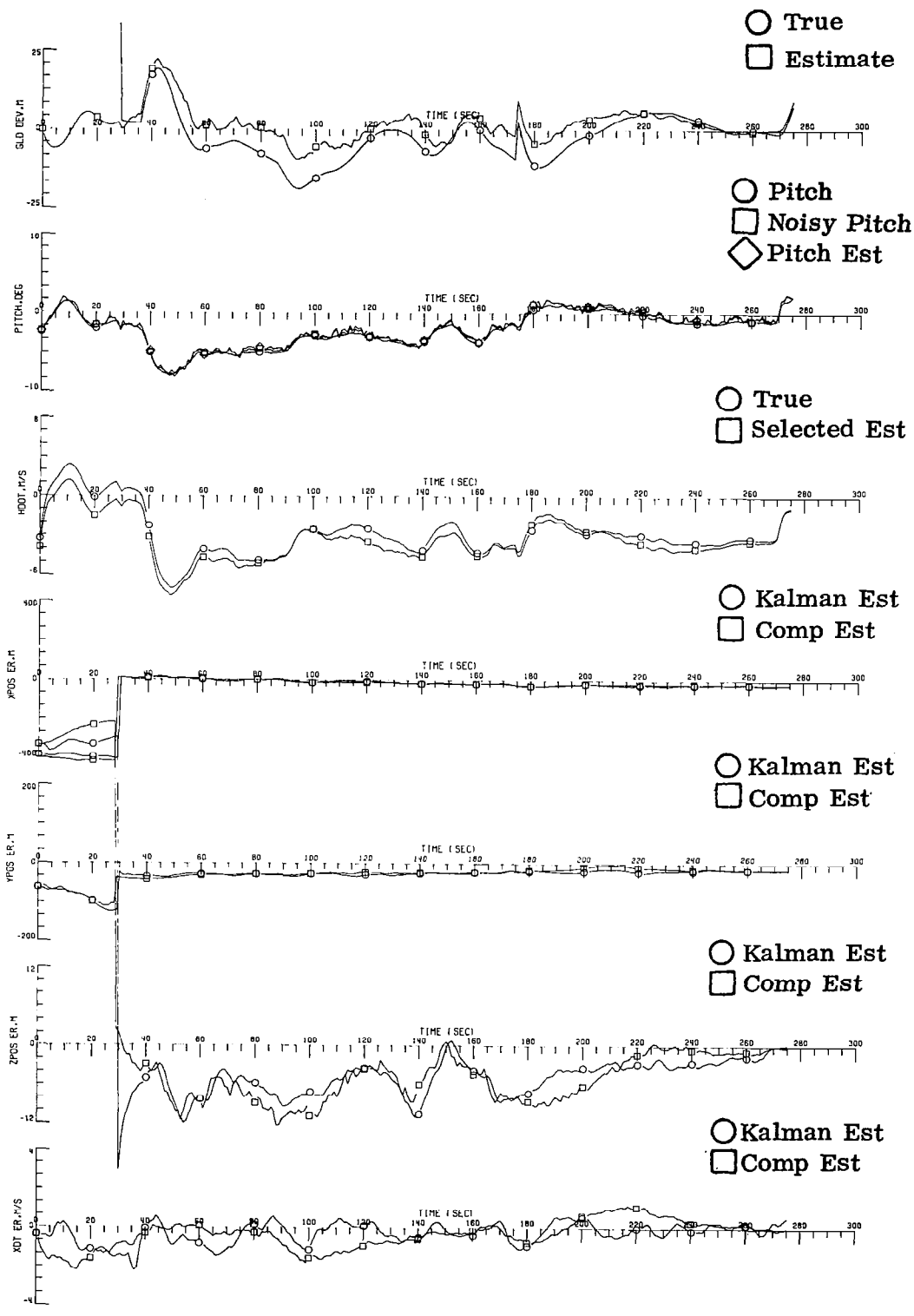

Figure 4(b). - Case 2.

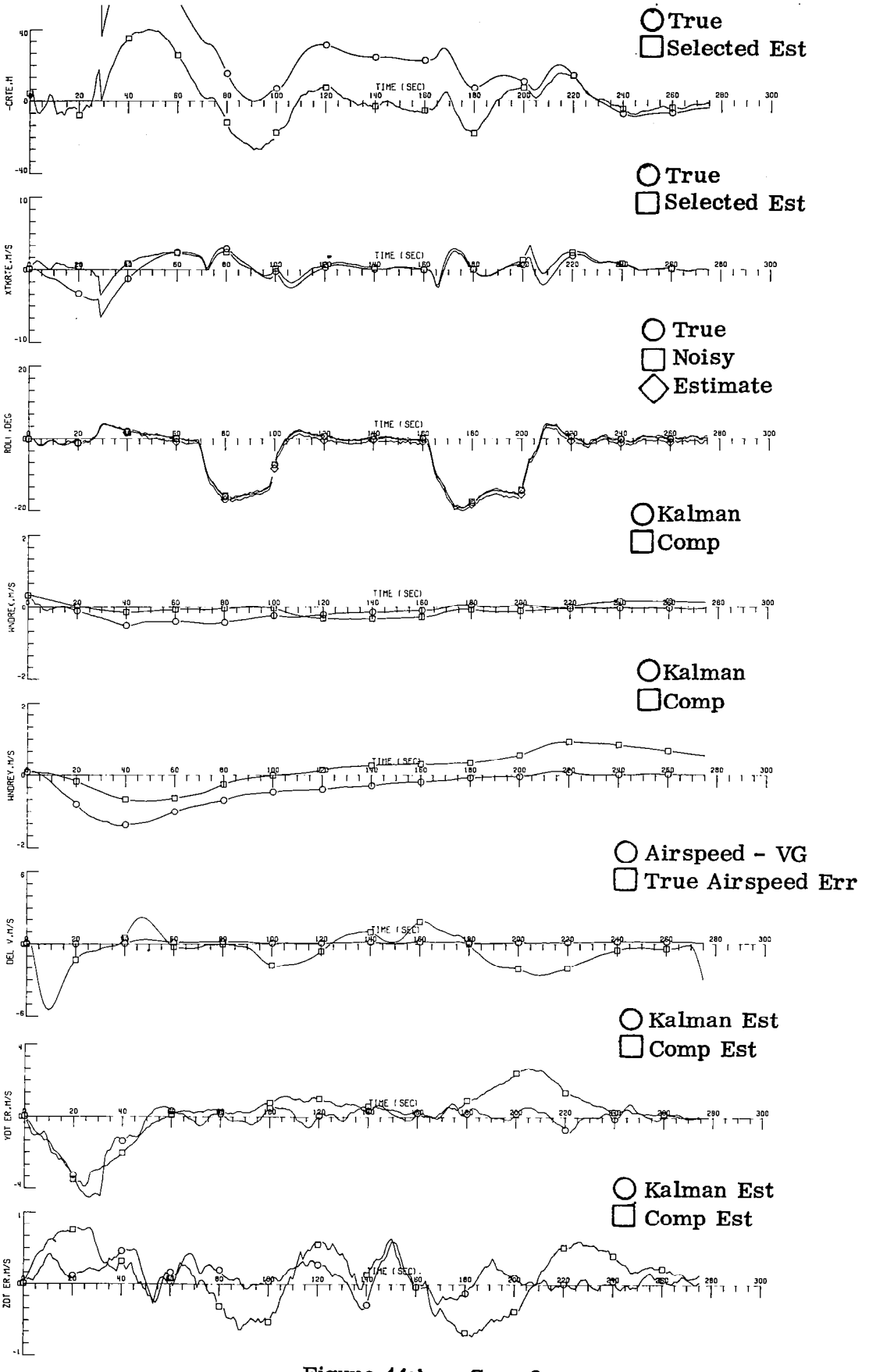

Figure 4(c). - Case 2.

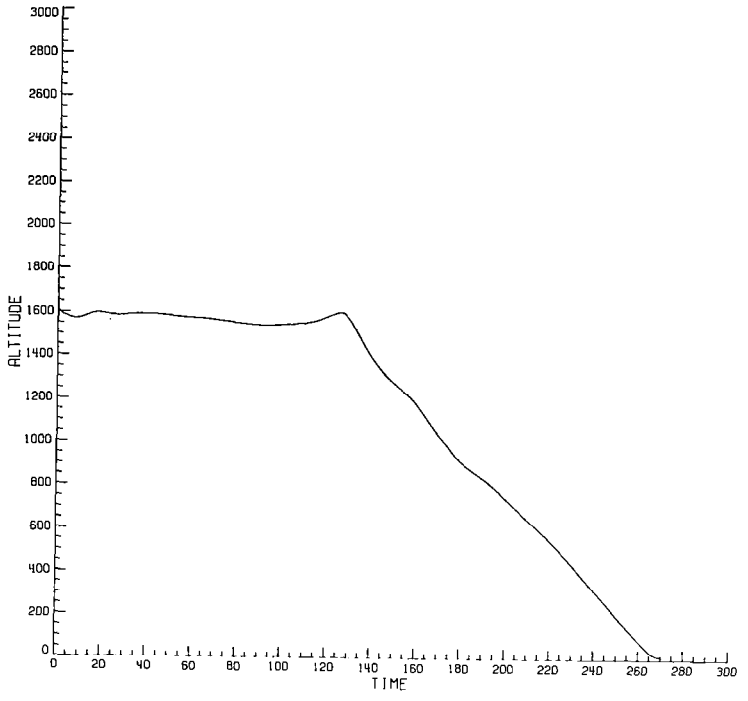

VERLIM = 914.4 m

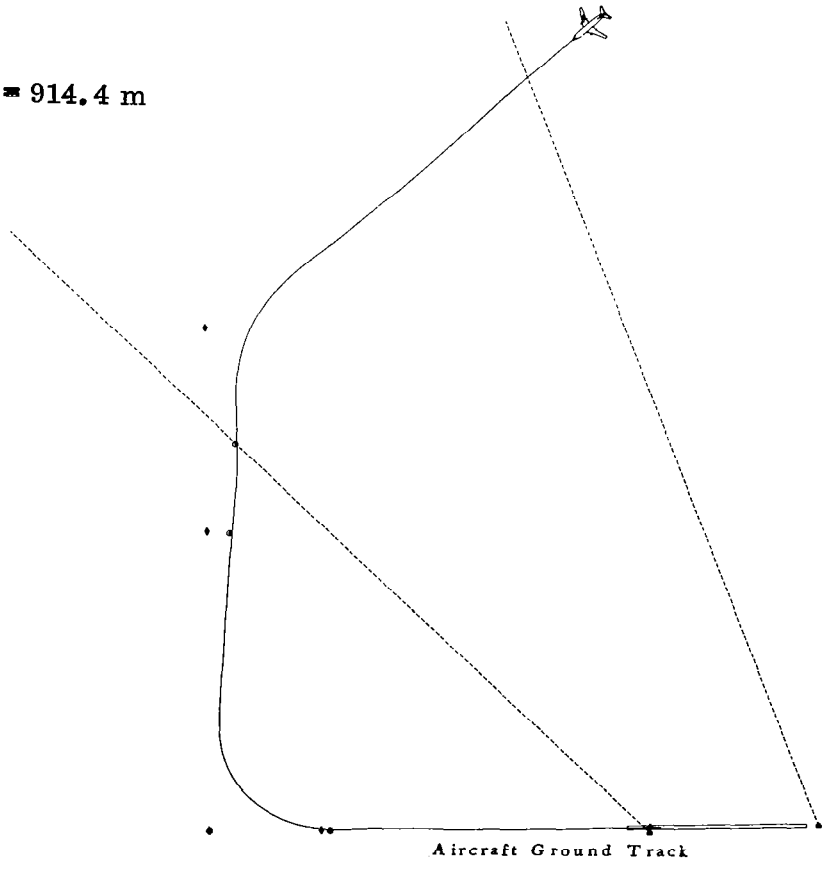

Final Distance = 2.35 Nautical Miles

Figure 5(a). - Case 3.

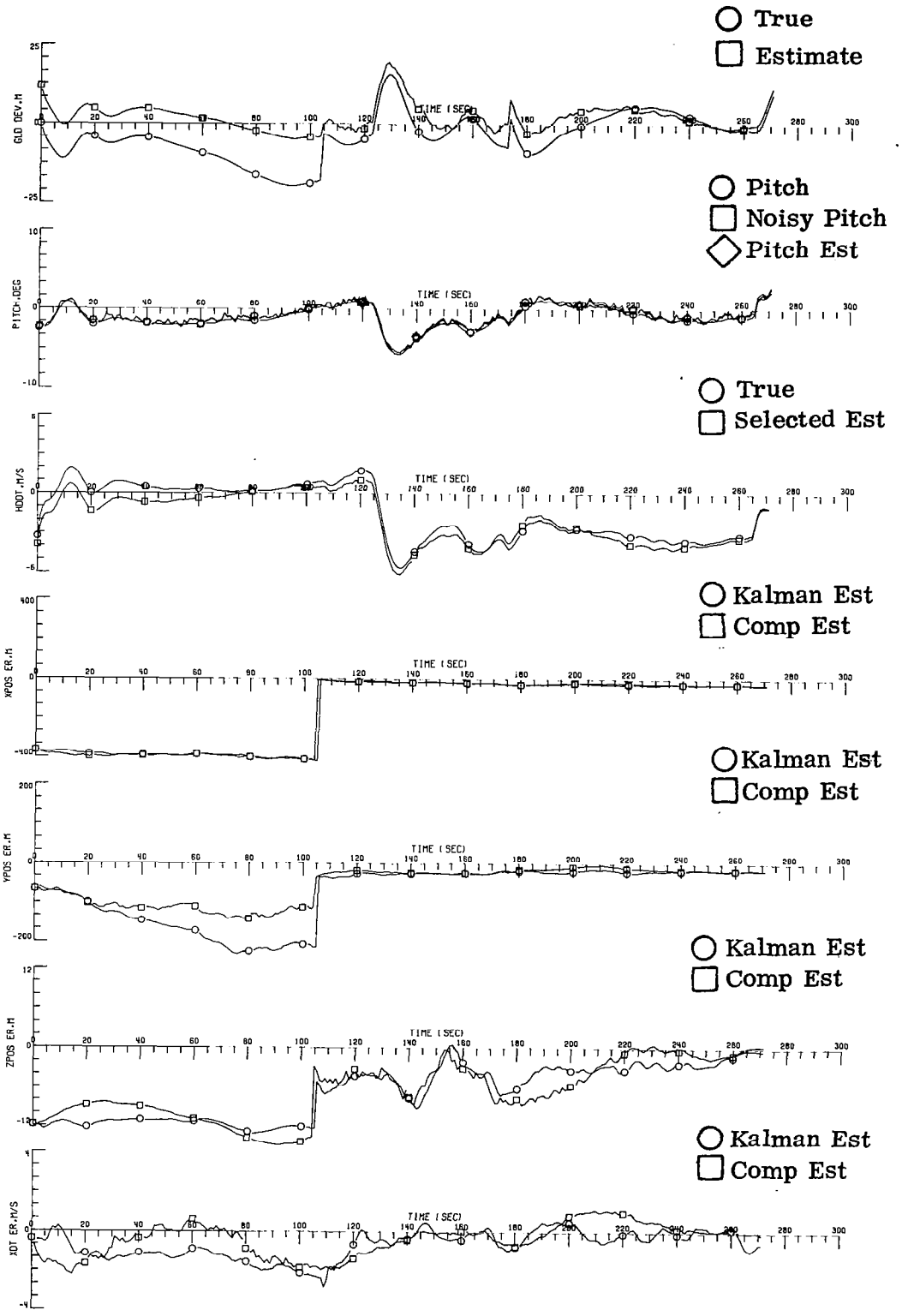

Figure 5(b). - Case 3.

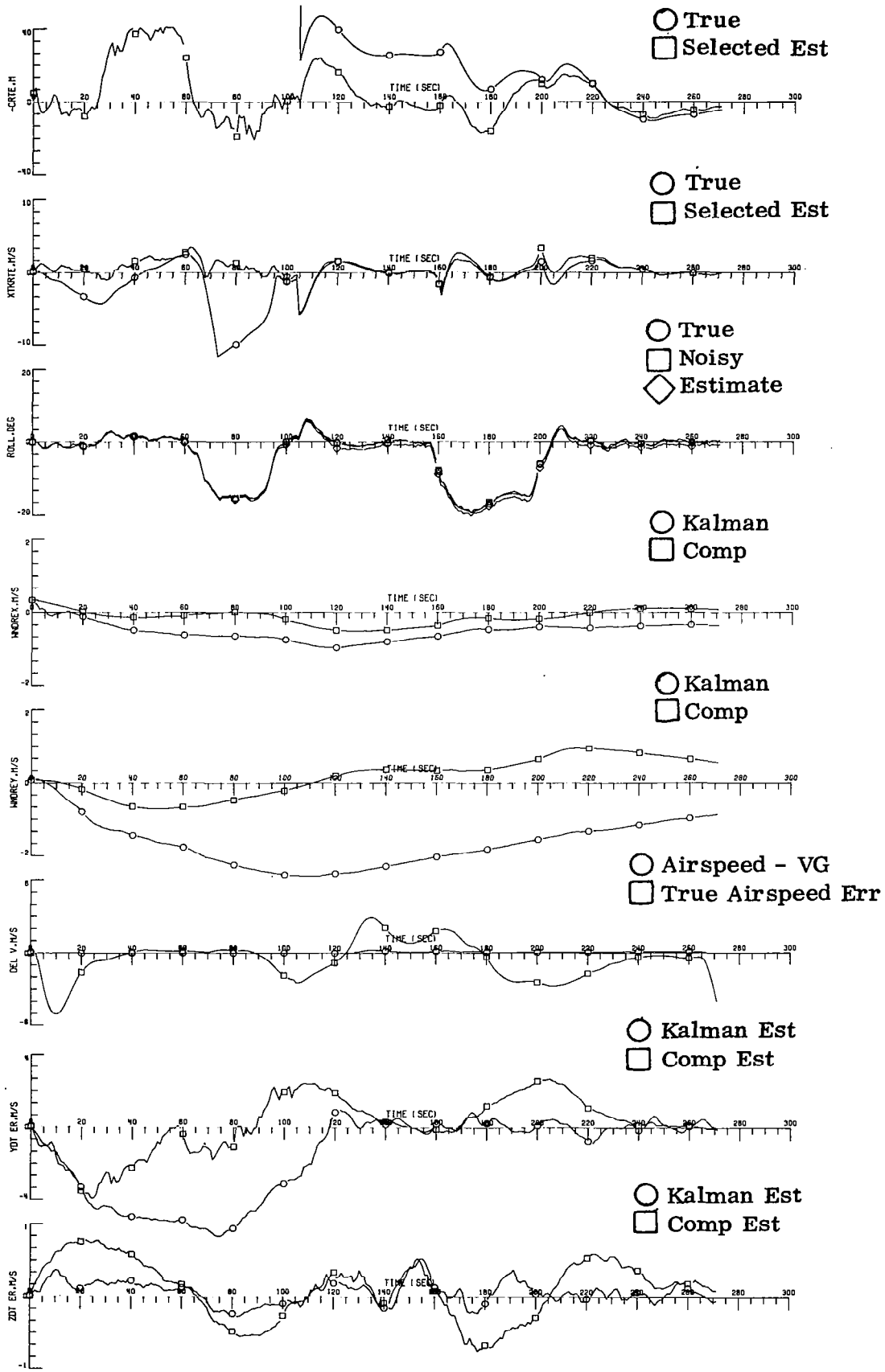

Figure 5(c). - Case 3.

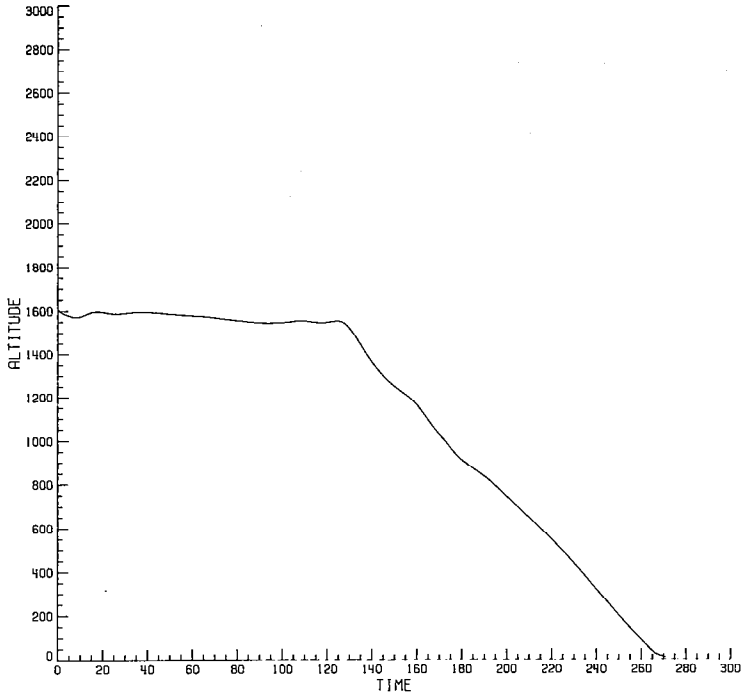

VERLIM = 1524 m

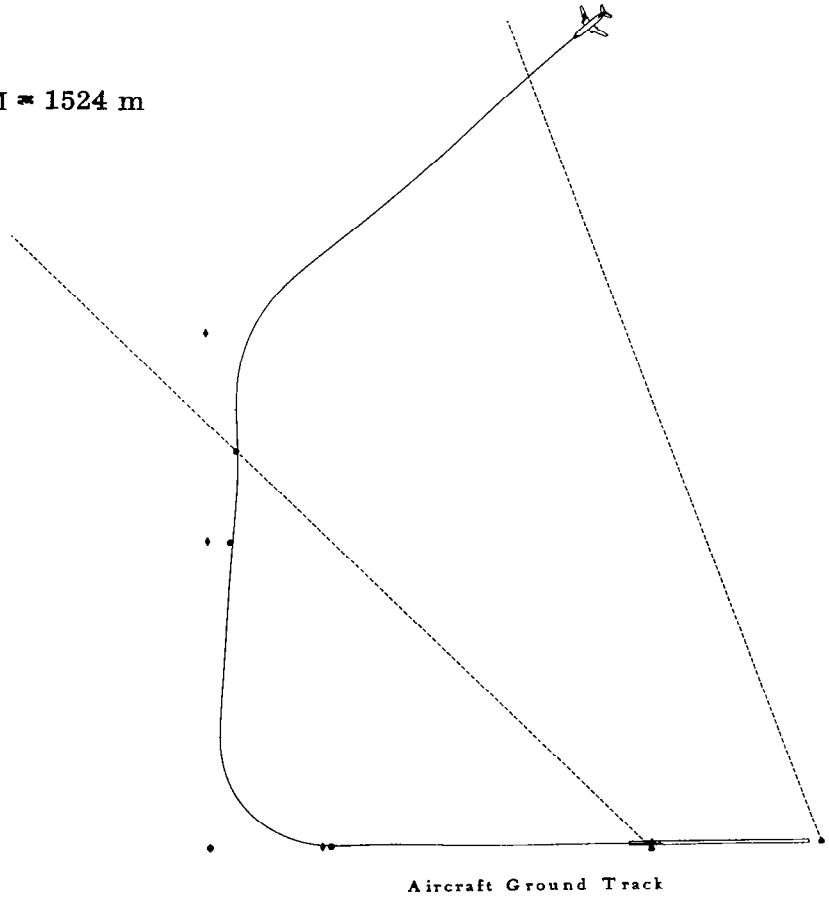

Final Distance = 2.35 Nautical Miles

Figure 6(a). - Case 4.

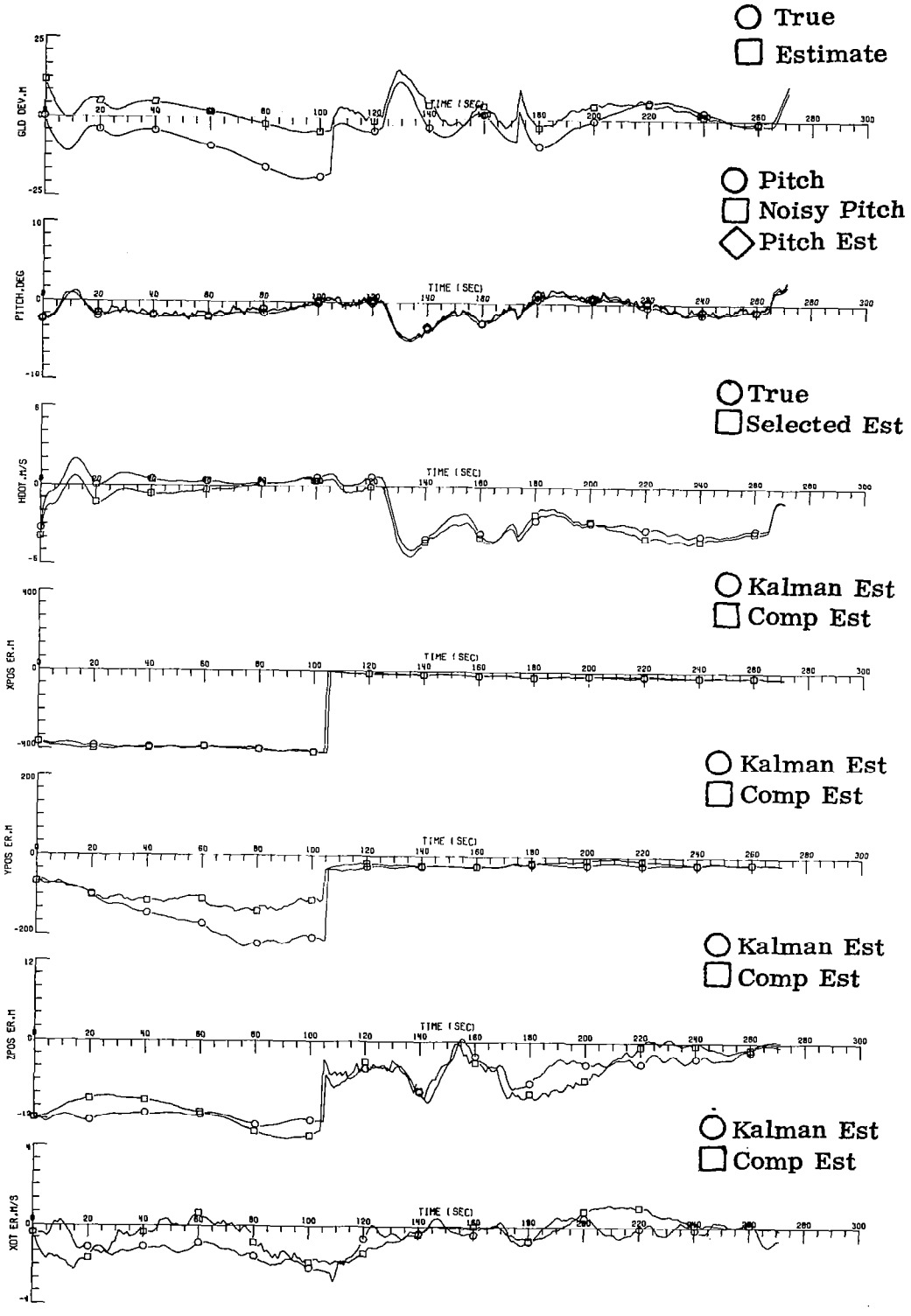

Figure 6(b). – Case 4.

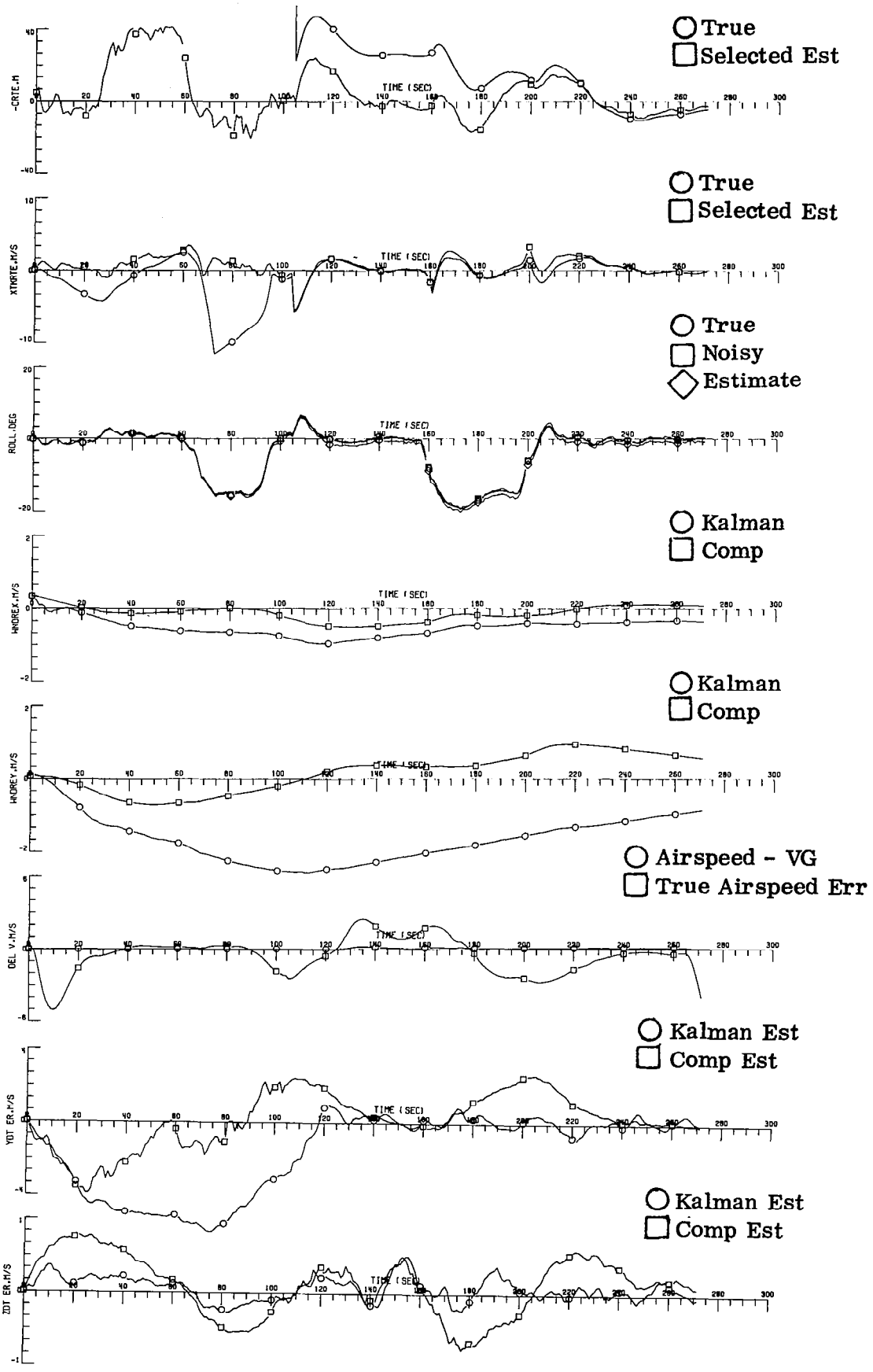

Figure 6(c). – Case 4.

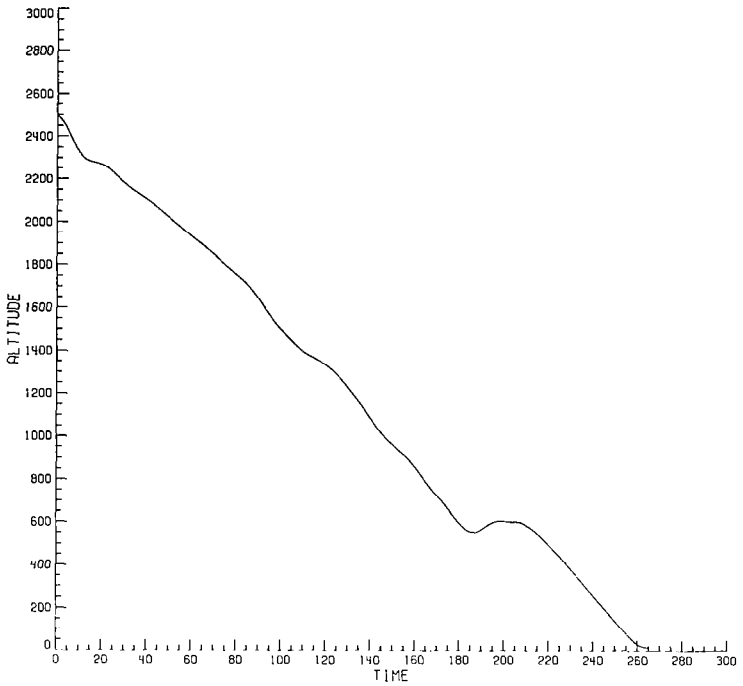

VERLIM = 914.4 m

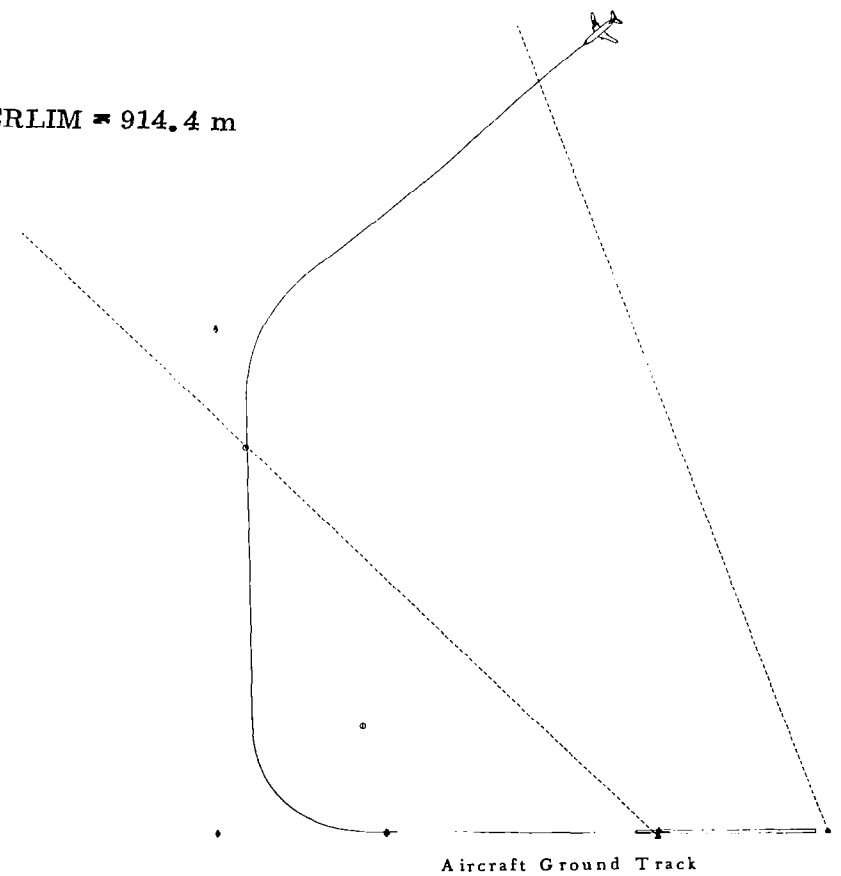

Final Distance = 2.00 Nautical Miles

Figure 7(a). - Case 5.

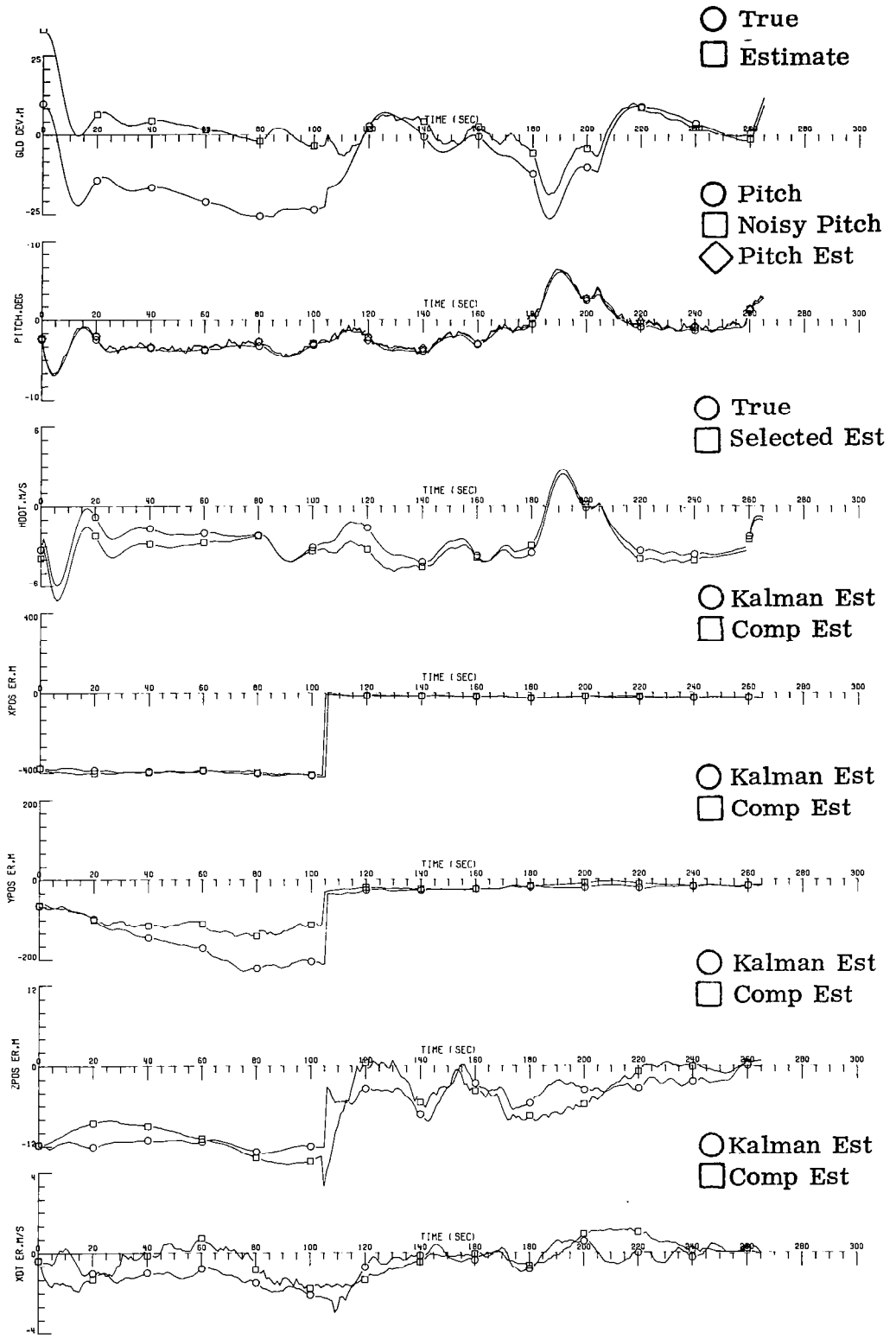

Figure 7(b). – Case 5.

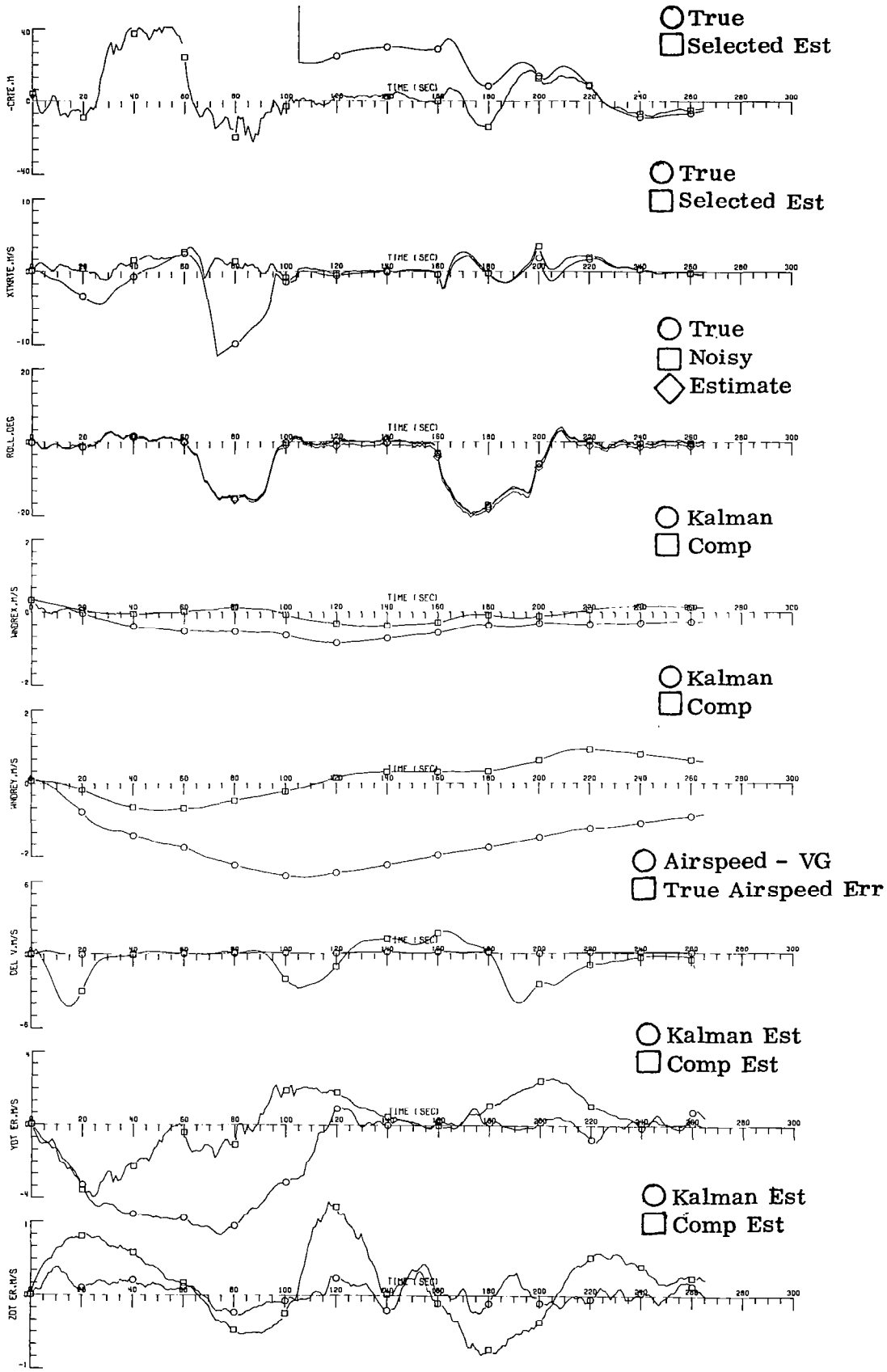

Figure 7(c). - Case 5.

1. Report No.	2. Government Accession No.	3. Recipient's Catalog No.
NASA CR-3574		

4. Title and Subtitle	5. Report Date
TERMINAL AREA AUTOMATIC NAVIGATION, GUIDANCE, AND CONTROL RESEARCH USING THE MICROWAVE LANDING SYSTEM (MLS) PART 4 - TRANSITION PATH RECONSTRUCTION ALONG A STRAIGHT LINE PATH CONTAINING A GLIDESLOPE CHANGE WAYPOINT	June 1982
	6. Performing Organization Code

7. Author(s)	8. Performing Organization Report No.
Samuel Pines	AMA 81-37
	10. Work Unit No.

9. Performing Organization Name and Address	11. Contract or Grant No.
Analytical Mechanics Associates, Inc. 17 Research Road Hampton, Virginia 23666	NAS1-15116

12. Sponsoring Agency Name and Address	13. Type of Report and Period Covered
National Aeronautics and Space Administration Washington, DC 20546	Contractor Report
	14. Sponsoring Agency Code

15. Supplementary Notes
Langley Technical Monitor: Richard M. Hueschen
Final Report - Part 4

16. Abstract

This report contains the algorithms necessary for constructing an aircraft flight path which contains a glideslope change at a waypoint which lies along a straight line. The report also contains the necessary algorithms to reconstruct the glideslope change waypoint along a straight line in the event the aircraft encounters a valid MLS update and transition in the terminal approach area. Results of a simulation of the Langley B737 aircraft utilizing these algorithms are presented. The method is shown to reconstruct the necessary flight path during MLS transition resulting in zero cross track error, zero track angle error, and zero altitude error, thus requiring minimal aircraft response.

17. Key Words (Suggested by Author(s))	18. Distribution Statement
Automatic Landing Navigation and Guidance Path Redesign MLS Navaids Transition	Unclassified - Unlimited Subject Category 04

19. Security Classif. (of this report)	20. Security Classif. (of this page)	21. No. of Pages	22. Price
Unclassified	Unclassified	42	A03

For sale by the National Technical Information Service, Springfield, Virginia 22161

NASA-Langley, 1982